KATSUSHIKA-HARP BRIDGE: VIBRATION MONITORING DURING EARTHQUAKES AND RESULTS

Theeraphong CHANPHENG, Eiichi SASAKI,
Hitoshi YAMADA, Hiroshi KATSUCHI and Kenta TAKAHASHI
Department of Civil Engineering, Yokohama National University, Japan

***ABSTRACT*:** Katsushika-Harp Bridge, the curved cable-stayed bridge in Tokyo, Japan, has been monitored for its vibration during earthquakes since 1987 until present. Initially, the main purpose of the monitoring was to observe its dynamic behaviors for design verification. At that time the significant use of vibration data for health monitoring of the large scale structures, which requires a lot of sensors, was not recognized. For these reasons, only a limited number of accelerometers were installed and only limited amount of data are available. Recently, the health condition of the Katsushika-Harp Bridge has become the major concerns. By using the existing limited data, this paper proposes the simple methods to detect *anomalies* in the *health condition*. The *health condition* is described by the Frequency Response Functions (FRFs). The *anomalies* are described by: (1) the changes of the degree of non-linearity obtained from the Hilbert transform of the FRFs, and (2) the changes of the natural frequencies extracted from the FRFs. The results from the five recent earthquake records are discussed. According to the results, the proposed methods show possibilities to detect the anomalies in the health condition even from the limited data. Nevertheless, the validity of the proposed methods as well as the damage simulation based on the finite element method need to be further investigated.

KEYWORDS: structural health monitoring, vibration of long-span bridges, frequency response function

1. INTRODUCTION

The Katsushika-Harp Bridge is a cable-stayed bridge located in Tokyo. It is a part of the Tokyo Metropolitan Expressway; however, it is very different from other cable-stayed bridges. The Katsushika-Harp Bridge has a unique curved-deck shape with the total length of girder 455 m (as shown in Fig.1 and Fig. 2). Due to the unique irregular shape, its dynamic characteristics especially during earthquake durations were carefully investigated.

Since the bridge was completed in 1987, the monitoring system (or the set of accelerometers with recording devices as shown in Fig.3) has been equipped for observing the dynamic response during earthquakes. The purpose of the monitoring was to verify the measured dynamic properties (e.g. natural frequencies and mode shapes) with the estimated dynamic properties used in the design stage. To measure only those properties, a set of sensors at some positions along the deck and towers was enough. Until these days, the monitoring system is still working and within these two decades, a large amount of vibration data has been recorded.

Recently in US and some European countries, the concept of *health monitoring* of large scale structures has been widely recognized (Sohn et al., 2003). The health monitoring is the monitoring

Figure 1 Katsushika-Harp Bridge

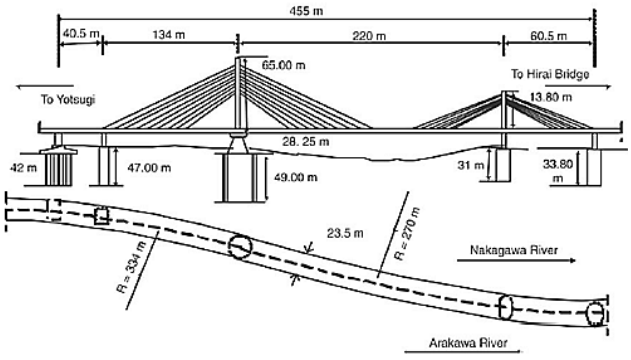

Figure 2 Dimension of the bridge (Siringoringo and Fujino, 2007)

system that monitors some specific quantities which can be inferred to the health or the damage condition of the structures. It appears to be complementary to the visual inspection. In the health monitoring system, the directly measurable quantities that represent the health condition or the damage of the structures will be firstly defined as the "features". Subsequently, the sensors will be installed to monitor the features. The anomalies in the health condition of the structures are the changes in the features when compared to their previous values. This monitoring system monitors *directly* the interested quantities without imposing any assumptions on the measured results. Then, a high reliability could be expected from this system.

Regarding the Katsushika-Harp Bridge, the monitoring system was, unfortunately, not the above case. The features that represent the health condition or the damage of the bridge were not previously defined. The system was designed to measure only the dynamic properties and there is only limited number of sensors at some positions of the bridge. However, it is possible to make this existing system to function as a *health monitoring* system. That is to

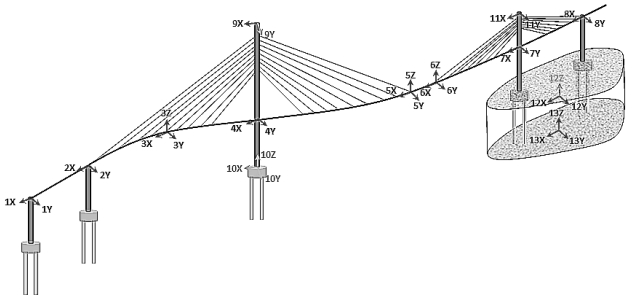

Figure 3 Sensors' Position and Directions

derive the "features" that expected to *indirectly* relate to the health condition by imposing some assumptions on the measure results. Certainly, unavoidable error as consequences of imposing the assumptions must affect the reliability of the monitoring system. The changes in the derived features when compared to their previous values may or may not indicate the anomalies in the condition of the bridge.

This paper proposes the simple methods to detect the anomalies in the health condition of the bridge. The "features" that *indirectly* relate the health condition are derived from the available vibration data. Although there are a lot of ways to analyze or interpret the vibration data, this paper use the *assumption* that the behaviors of the bridge can be fully described by the Frequency Response Functions Matrix (from now on, will be simply called FRFs). The FRFs are practically used in mechanical engineering community for describing the characteristics of structures from the input (forces) signals and output (responses) signals (Ewins, 2000). The "features" derived from the FRFs are used to indicate the anomalies in the health condition. In this paper, the proposed method utilizes two following features from the FRFs:

(1) The degrees of non-linearity in vibration which are *assumed* to represent the non-linearity of vibration behavior. This feature is derived from the Hilbert transform of the FRFs.

(2) The natural frequencies obtained from the

decomposition of the FRFs which are *assumed* to represent indirectly the support conditions or the stiffness of the bridge.

The changes in the above features are expected to indicate the anomalies in the health condition of the bridge. The expected anomalies may be abruptly changes or gradually changes. The abruptly changes may occur after one event such as an extremely strong earthquake. The gradually changes may be the results of the degradation of the structural materials.

By using the above method, the methods and the results from all available data, and the validity of the methods will be discussed.

2. DESCRIPTION OF THE BRIDGE

The dimension of the Katsushika-Harp Bridge is shown in Fig.2 (Siringoringo and Fujino, 2007), and the sketch of monitoring system is shown in Fig.3. The detail of the bridge and its monitoring system will be described in this section.

2.1 Girder and Towers

The bridge's girder is made from steel with the width of 23.5 m and the total length of 455 m, consisting of 220 m main span, and three side spans of 40.5, 134 and 60.5 m. From plan view, the girder is curved like 'S' with radii 334 m and 270 m. This part of the bridge is the main interest of this paper.

There are two rectangular towers made from steel. The main tower is 65 m in height and 3m in width. Another tower is 13.8 m in height and 2.5 m in width.

2.2 Monitoring System

The monitoring system (in Fig.3) consists of 32 channels of accelerometers permanently installed on the bridge. The sensors were installed at 12 locations along the girder, towers, and foundations. On the girder, the sensors were installed along the girder's centerline. The sensors measure accelerations in longitudinal, horizontal, and vertical directions with a sampling rate 100 Hz during the earthquake durations. The directions are denoted by X: global longitudinal direction, Y: global horizontal direction, and Z: vertical direction. It is also important to note that some sensors are clearly malfunctioning and data from some sensors are significantly corrupted by noise.

2.3 Seismic Records

The acceleration records of ground motions and the responses from five earthquakes are available as shown in Table 1. The examples of the time-histories are shown in Fig.4-8.

Table1 List of seismic records in the analysis

No.	Earthquake (Trigger Time)	Magnitude (Mj)	Total Length (sec)
I	Nov 3, 2003 (12:37)	6.3	45.32
II	May 12, 2003 (00:57)	5.3	33.50
III	Oct 15, 2003 (16:30)	5.1	39.50
IV	Jul 23, 2005 (16:34)	6.0	45.00
V	Aug 16, 2005 (11:46)	7.2	70.25

(Data from http://www.jma.go.jp)

2.4 Bridge's physical properties and modeling

In this paper, the physical properties of the bridge are not yet available. From this reason, the finite element model of the bridge cannot be created. The dynamic properties of the bridge also cannot be predicted. The complicated damage scenarios of the bridge cannot be performed as well.

Unlike the above model-based method like finite element method, another way to describe the characteristics of the bridge without knowing the physical properties is to use a non-model based method. There are many kinds of non-model based methods that map the input-output relationship of a structure, such as Auto-Regressive Exogenous (ARX) model, state-space model, neural network model, and Frequency Response Function (FRF), etc.

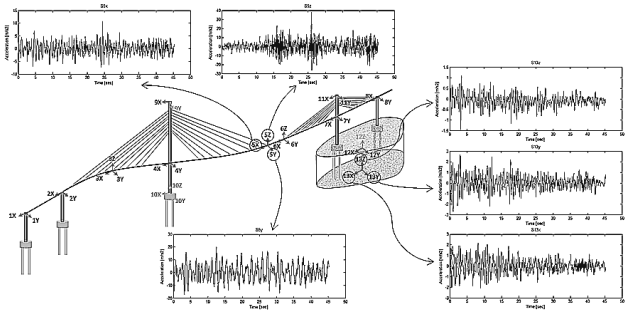

Figure 4 Time history of earthquake I

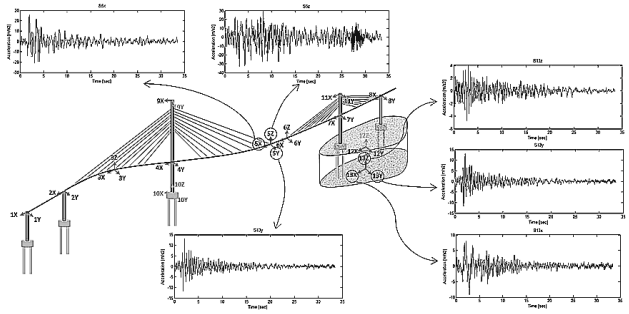

Figure 5 Time history of earthquake II

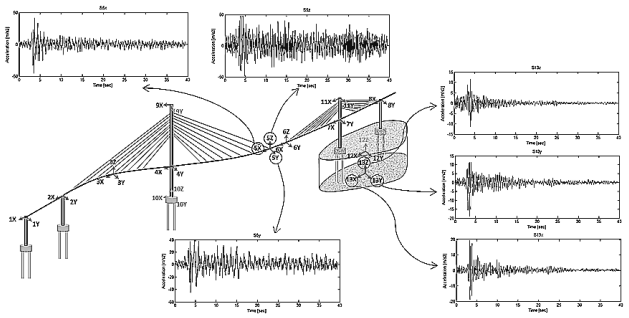

Figure 6 Time history of earthquake III

The last one was selected for this paper because it is possible to be decomposed into physical related parameters (modal parameters).

3. METHODOLOGY

This section introduces the basic idea of the FRFs and their derived features, i.e., the degrees of non-linearity and the natural frequencies.

3.1 Frequency Response Functions (FRFs)

Assuming that the structure is a *linear time invariant* system, the equation of motion of the structure in time-domain becomes

$$\mathbf{M}\ddot{\mathbf{y}}(t)+\mathbf{C}\dot{\mathbf{y}}(t)+\mathbf{K}\mathbf{y}(t)=\mathbf{u}(t) \qquad (1)$$

where **M** is the structural mass matrix, **C** is the damping matrix, **K** is the stiffness matrix, t is time, **u** is the external force vector (input vector) applying to

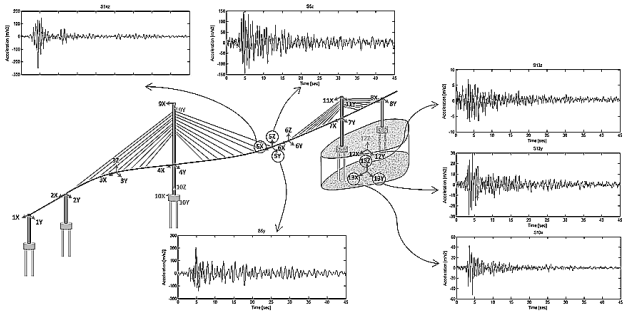

Figure 7 Time history of earthquake IV

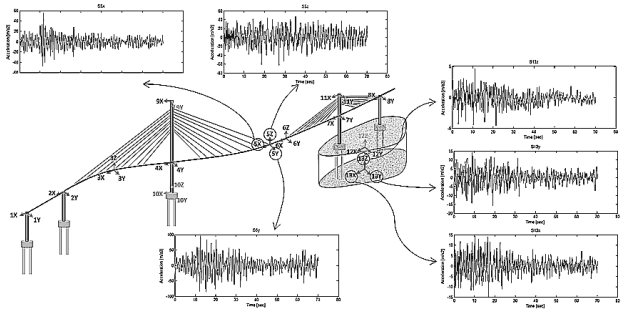

Figure 8 Time history of earthquake V

the structure, and **y** is the displacement vector (output vector). Taking Laplace transform on both sides of the equation and then evaluating the value on the imaginary axis of the Laplace domain (or s domain), the above equation can be rewritten in a form of Fourier transform (or frequency domain) of **u** and **y** as

$$\mathbf{Y}(\omega)=\boldsymbol{\alpha}(\omega)\mathbf{U}(\omega) \qquad (2)$$

in which

$$\boldsymbol{\alpha}(\omega)=\left(-\omega^2\mathbf{M}+i\omega\mathbf{C}+\mathbf{K}\right)^{-1} \qquad (3)$$

where ω denotes the frequency and $i^2=-1$; $\mathbf{Y}(\omega)$ and $\mathbf{U}(\omega)$ are the Fourier transform of $\mathbf{y}(t)$ and $\mathbf{u}(t)$ respectively.

In the above equation, the function $\boldsymbol{\alpha}(\omega)$ is called the basic form of the FRF since it describes the behavior of the structures in the frequency-domain. It represents the relationship between external forces and measured displacement. However, if the accelerations are measured instead of the displacements, the Eq.(2) will be

$$\ddot{\mathbf{Y}}(\omega)=\mathbf{H}(\omega)\mathbf{U}(\omega) \qquad (4)$$

where

$$\mathbf{H}(\omega) = -\omega^2 \boldsymbol{\alpha}(\omega) \quad (5)$$

The function $\mathbf{H}(\omega)$ is an alternative form of the FRF (Ewins, 2000). Sometimes it was called the inertance of accelerance, but in this paper will be referred as the FRF. The FRF contains the information of structural mass, damping, and stiffness. Theoretically, it is enough to describe structural behavior by using only this function.

To compute the FRF is not difficult. The required information is the Fourier transforms of the earthquake ground motions (input) and of the bridge's accelerations (output). The FRF can be calculated from

$$\mathbf{H}(\omega) = \left[\mathbf{Y}(\omega)\mathbf{U}(\omega)^*\right]\left[\mathbf{U}(\omega)\mathbf{U}(\omega)^*\right]^{-1} \quad (6)$$

where * denotes the complex conjugate transpose of the matrix. When the function $\mathbf{H}(\omega)$ is evaluated, its variance along the frequency is removed by using the well known Welch's average. However, it is important to note that the above equation will give a reliable result if the input $\mathbf{U}(\omega)$ is rich in frequencies. Otherwise, the inverse operation may yield some errors.

After computing the FRFs, the "features" can be later evaluated. The following section describes the features derived from the FRFs.

3.2 The degree of non-linearity

The non-linearity indirectly indicates the health condition of a structure. There were many reports showing that when a structure behaves non-linearly, that may be the results of damages or changes in the health condition (Sohn et al., 2003).

In this paper, the degree of non-linearity can indicates how much the actual structural behavior is different from the assumed linear behavior in the Eq.(1). Changing abruptly or gradually from lowly to highly non-linear behavior may be considered as the anomalies.

3.2.1 Extraction of the degree of non-linearity

The degree of non-linearity can be calculated from the FRFs. It exploits the fact that the FRF of a linear system is invariant under a Hilbert transform (Kerschen et al, 2006). For an ideally linear system, the FRF composes of real and imaginary parts. Both parts behave like a linear analytic function which preserves a unique relationship between the real and the imaginary parts. The real part of the FRF can be generated from its imaginary part (and vice versa) by the Hilbert transform.

The Hilbert transform of the FRF is defined by (Simo and Tomlinson, 1984)

$$\mathscr{H}\left[\mathbf{H}(\omega)\right] = -\frac{1}{\pi i} PV \int_{-\infty}^{\infty} \frac{\mathbf{H}(\Omega)}{\omega - \Omega} d\Omega \quad (7)$$

where $\mathscr{H}$ denotes the Hilbert transform operator and PV denotes the Cauchy Principal Value of the integral.

For a linear system in which the output can be described by the convolution of the input with the unit-impulse response function, it has been verified that the following relationships hold true (Simo and Tomlinson, 1984):

$$\mathscr{H}\left[\mathbf{H}(\omega)\right] = \mathbf{H}(\omega) \quad (8)$$

in other word,

$$\mathscr{H}\left[\mathrm{Re}\left(\mathbf{H}(\omega)\right)\right] = \mathrm{Im}\left(\mathbf{H}(\omega)\right) \quad (9)$$

$$\mathscr{H}\left[\mathrm{Im}\left(\mathbf{H}(\omega)\right)\right] = \mathrm{Re}\left(\mathbf{H}(\omega)\right) \quad (10)$$

The above equations mean that the Hilbert transform of the real part is equal to the imaginary part, and the Hilbert transform of the imaginary part is equal to the real part.

3.2.2 Detection of the anomalies

If the shapes of the FRFs of any structures does not change after the Hilbert transform, the structures behave linearly like Eq.(1). However, if the shapes of the FRFs completely change after the Hilbert

transform, the structures behave non-linearly.

The similarity between the FRF before and after the Hilbert transformation may be a good measure for the degree of non-linearity. The similarity is expressed by a frequency-dependent coherence function (COH) as (Rauch, 1992)

$$\mathrm{COH}(\omega)=\frac{\left|\mathscr{H}\left[\mathbf{H}(\omega)\right]^{*}\mathbf{H}(\omega)\right|^{2}}{\left|\mathscr{H}\left[\mathbf{H}(\omega)\right]\right|^{2}\left|\mathbf{H}(\omega)\right|^{2}}\leq 1.0 \tag{11}$$

The above function varies from 0 for the completely non-linear behavior, to 1 for the perfectly linear behavior. The above coherence function is the degree of non-linearity in this paper.

For each earthquake, if there were no anomalies in the health condition, the degree of non-linearity at certain frequencies should not significantly change. However, the significant changes in the degree of non-linearity can indicate that something in the structure has changed but cannot identify what kind of situation or changes occurred. This is the limitation of the method.

3.3 The changes in natural frequencies

As mentioned, the changes of the degree of non-linearity could indicate the anomalies of the structure. However, it is not possible to understand what happened to the structure. The link that can relate the FRFs to the physical properties of the structure is the modal representation.

The modal representation (or modal analysis) decomposes the measured FRF into a set of independent modes described by their modal parameters. The parameters consist of natural frequencies, modal shapes, and modal damping. Theoretically, the modal parameters are enough to describe the characteristics of the structure. The changes in modal parameters indicate the changes in the physical properties of the structure. The changes in natural frequencies, could detect the changes in support condition and/or changes in mass or stiffness. The changes in modal shapes (or modal shapes' curvature) and modal damping also indicate the damages as well (Sohn et al., 2003).

Regarding the Katsushika-Harp Bridge, since a limited number of sensors are available, the calculated modal shapes are not much reliable compared to the natural frequencies which could be obtained directly from the peaks of the FRF. In addition, there was a report showing that the modal dampings of the Katsushika-Harp Bridge are very scattered even the advanced time-domain identification algorithm was used (Siringoringo and Fujino, 2007). From these reasons, the reliable parameters are only the natural frequencies. This paper uses the natural frequencies as a feature.

3.3.1 Extraction of the natural frequencies

To extract the natural frequencies (and mode shapes together) from the measured FRFs, the Complex Mode Indicator Function (CMIF) will be used (Ewins, 2000).

Assuming that a FRF can be decomposed into independent modes, by using the singular value decomposition (SVD), the FRF at each frequency in the consideration can be decomposed into

$$\mathbf{H}(\omega)=\mathbf{\Phi}(\omega)\mathbf{\Sigma}(\omega)\mathbf{\Psi}(\omega)^{*} \tag{12}$$

in which the matrix $\mathbf{\Phi}(\omega)$ and $\mathbf{\Psi}(\omega)$ represent, respectively, the output and input orthonormal basis vector directions for $\mathbf{H}(\omega)$. The matrix $\mathbf{\Sigma}(\omega)$ contains the singular values of the matrix $\mathbf{H}(\omega)$. In general, the fist singular value dominates all the others. Keeping only the most significant component, the matrix $\mathbf{H}(\omega)$ can be approximated by

$$\mathbf{H}(\omega)\approx\sigma_{1}(\omega)\mathbf{\Phi}_{1}(\omega)\mathbf{\Psi}_{1}(\omega)^{*} \tag{13}$$

where $\mathbf{\Phi}_1(\omega)$ and $\mathbf{\Psi}_1(\omega)$ are the first column vectors in $\mathbf{\Phi}(\omega)$ and $\mathbf{\Psi}(\omega)$ respectively. The $\sigma_1(\omega)$ is the first maximum singular value in the matrix $\mathbf{\Sigma}(\omega)$. The frequency-dependent $\sigma_1(\omega)$ is called the complex mode indicator function (CMIF).

In mathematical sense, the $\sigma_1(\omega)$ or CMIF is

actually the representative of all elements in the $\mathbf{H}(\omega)$ matrix. The peaks on the CMIF are the natural frequencies. The vectors $\mathbf{\Phi}_1(\omega)$ at the peaks of the CMIF are the modal shape vectors at the frequencies of those peaks. The modal vectors are described by complex quantities relating both amplitudes and phases.

However, distinguishing a peak in the CMIF subjectively is rather difficult. A criterion for this purpose is Modal Assurance Criteria (MAC) which identifies similarity of modal shape vectors between two adjacent frequencies.

$$\mathrm{MAC}(\omega_i) = \frac{\left|\mathbf{\Phi}_1(\omega_{i-1})^* \mathbf{\Phi}_1(\omega_i)\right|^2}{\left|\mathbf{\Phi}_1(\omega_{i-1})\right|^2 \left|\mathbf{\Phi}_1(\omega_i)\right|^2} \le 1.0 \tag{14}$$

The frequencies at the peaks where the mode shape vectors are stable (i.e. MAC is between 0.8 and higher) are considered as the natural frequencies (Michel et al, 2007).

3.3.2 Detection of the anomalies

From a record of an earthquake, the above method extracts a set of natural frequencies in longitudinal, horizontal, and vertical directions and put into the feature matrix **F** like

$$\mathbf{F} = \begin{bmatrix} \langle \omega_X \rangle & \langle \omega_Y \rangle & \langle \omega_Z \rangle \end{bmatrix} \tag{15}$$

where $\langle\ \rangle$ indicate a row vector of the natural frequencies of each directions. When more records are available (N records), a set of natural frequencies from each record can be augmented into

$$\mathbf{F} = \begin{bmatrix} \langle \omega_{X1} \rangle & \langle \omega_{Y1} \rangle & \langle \omega_{Z1} \rangle \\ \langle \omega_{X2} \rangle & \langle \omega_{Y2} \rangle & \langle \omega_{Z2} \rangle \\ \vdots & \vdots & \vdots \\ \langle \omega_{XN} \rangle & \langle \omega_{YN} \rangle & \langle \omega_{ZN} \rangle \end{bmatrix} \tag{16}$$

The idea is of the comparison comes from the fact that if the structural properties after each earthquake do not change, all the values in any rows in **F** are exactly identical. Then the rank of the feature matrix **F** must be 1. However, if the anomalies occurred, some elements in the augmented row will be different from all the others and the rank must be more than 1. Nevertheless, even if the structure is healthy, the natural frequencies extracted from each earthquake will generally not be exactly the same value in mathematical sense. It is better to count the number of the significant singular values of the matrix instead of calculating the rank directly. Having more than one significant singular value indicates that some anomalies occurred. The ratio of the first singular value and the second value is an appropriate index for this case. The healthy structure will have very high ratio whereas the damaged structure will have lower ratio.

The anomalies to be detected are the changes in the support conditions and the changes in stiffness of the structure. However, it is known that the natural frequencies are not sensitive to local or small damages. Only the anomalies in the global behavior of the bridge are expected to be detected.

3.4 Testing the proposed methods

Actually, to verify how the proposed methods can detect the anomalies is to test the following test cases:

(1) If the bridge is still healthy, the proposed methods should extract the same value of features from all earthquakes.

(2) If the bridge is not healthy, the proposed methods should identify that there are changes in the value of the features.

The Katsushika-Harp Bridge, even today, is still healthy. The proposed methods in this paper should identify that the bridge is still healthy. That means all the derived quantities must be theoretically identical regardless of any earthquake records, as the test case (1). However, the test case (2) cannot be performed since lacking of the physical model/finite element model of the bridge.

The degree of non-linearity proposed in this

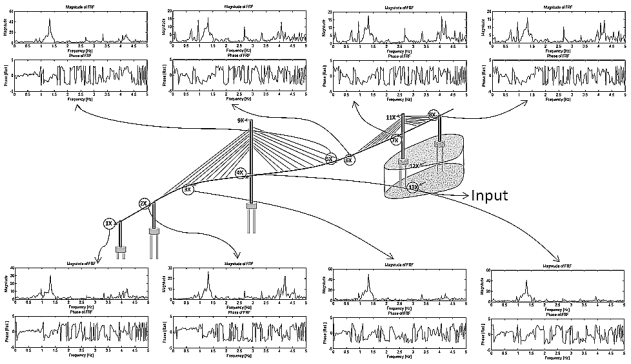

Figure 9 FRF X-Direction of earthquake I

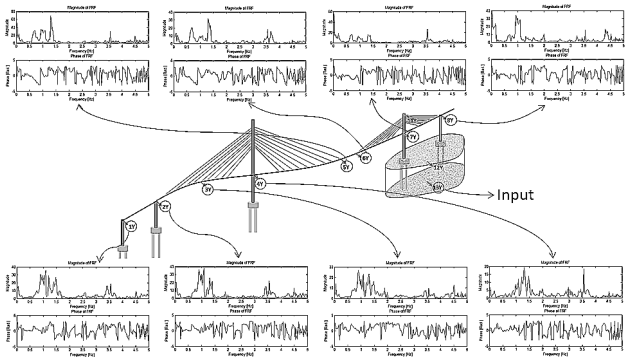

Figure 10 FRF Y-Direction of earthquake I

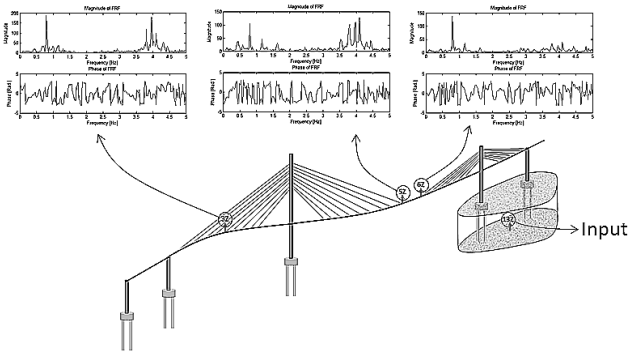

Figure 11 FRF Z-Direction of earthquake I

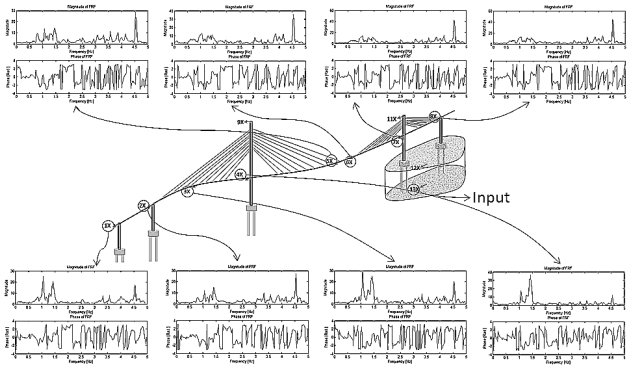

Figure 12 FRF X-Direction of earthquake II

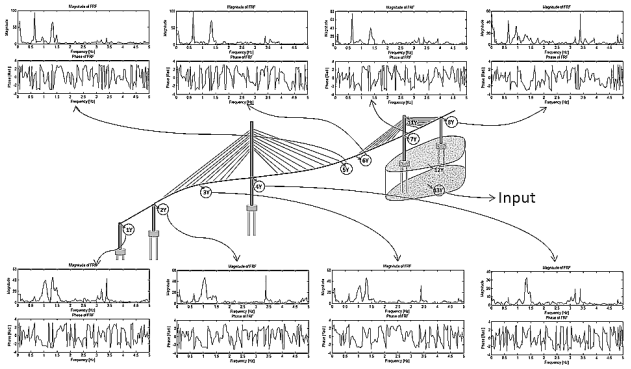

Figure 13 FRF Y-Direction of earthquake II

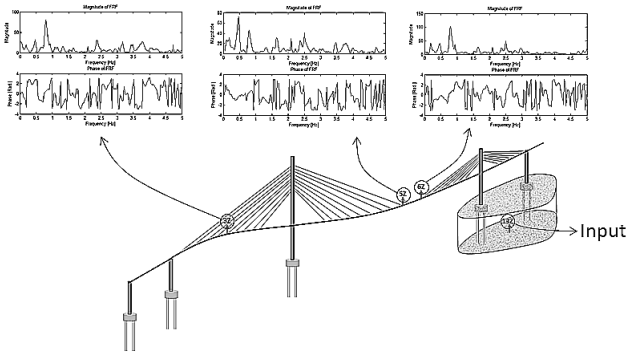

Figure 14 FRF Z-Direction of earthquake II

paper can test only the case (1) whereas the natural frequencies can test both cases. But only simple damage simulation can be done for the method that uses the natural frequencies.

4. RESULTS OF THE PROPOSED METHODS

In this paper, the frequency range that is of interest is limited to 0 to 5 Hz, which governs all the global vibration characteristics of the bridge. The following sub-sections are the results and their discussions.

4.1 FRFs

The FRFs of all earthquake records have been computed. The example of the FRFs in longitudinal (X), horizontal (Y), and vertical (Z) of the earthquake I and earthquake II are shown in Fig.9-14. The figures show both amplitudes (upper) and phases (lower) on each measurement point on the girder. From the figures, there are a lot of FRFs plot of each direction and each earthquake record. However, plotting the CMIF is easier to understand. The CMIF simplifies (or average) the FRFs into a simple form. The CMIFs from each direction of each earthquake are shown in Fig. 15.

Fig. 15 shows that the CMIFs from each earthquake are similar in the peak positions, but are

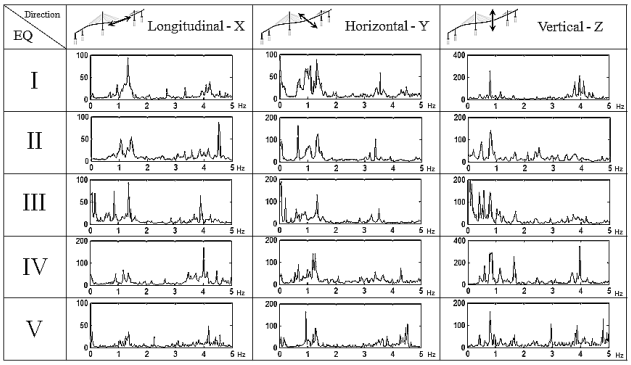

Figure 15 Comparison of the CMIF

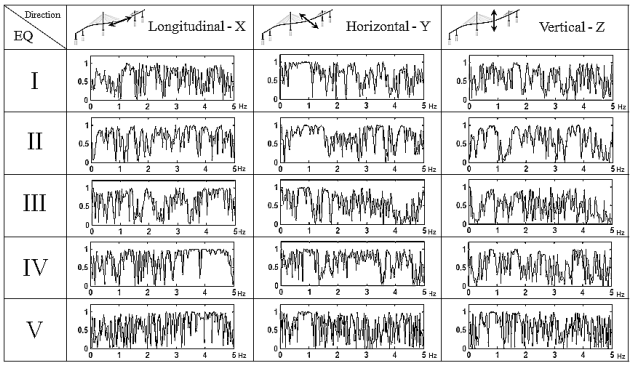

Figure 16 Comparison of the COH function

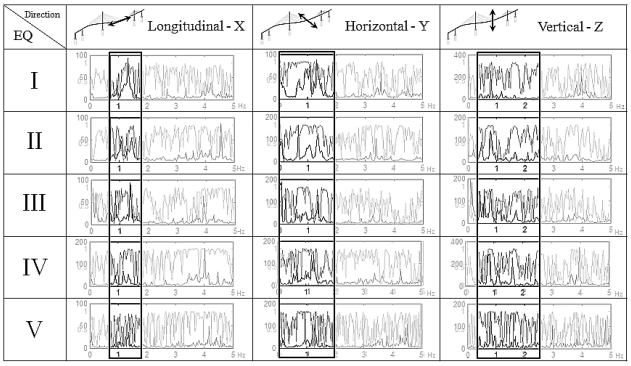

Figure 17 Comparison of the COH and CMIF

not exactly identical to each other. Actually, the FRFs/CMIFs which indicate the structure's properties should not be independent on the earthquakes. The variation among CMIFs may be the results from (1) noise contaminated in the measured data and (2) the input signal (ground motion records) may not be rich in frequencies so that the inverse operation in the Eq.(6) yields some errors.

The next subsection will describe the use of the computed FRFs for detecting the anomalies in the health condition.

4.2 Degree of nonlinearity

From the FRFs, the Hilbert transform has been

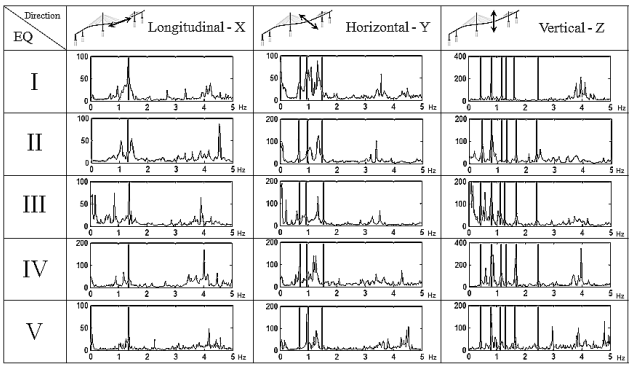

Figure 18 Natural Frequencies at the vertical lines

Direction / EQ	Longitudinal - X	Horizontal - Y	Vertical - Z
I	1.328 Hz	0.703, 0.938, 1.484 Hz	0.430, 0.801, 1.172, 1.309, 1.641, 2.461 Hz
II	1.387 Hz	0.645, 0.957, 1.484 Hz	0.469, 0.801, 1.152, 1.309, 1.641, 2.363 Hz
III	1.367 Hz	0.684, 0.918, 1.543 Hz	0.410, 0.801, 1.133, 1.270, 1.699, 2.422 Hz
IV	1.348 Hz	0.664, 0.996, 1.465 Hz	0.410, 0.801, 1.133, 1.387, 1.641, 2.461 Hz
V	1.357 Hz	0.625, 0.938, 1.543 Hz	0.430, 0.801, 1.172, 1.338, 1.670, 2.451 Hz

Figure 19 Extract Natural Frequencies

Direction / EQ	Longitudinal - X	Horizontal - Y	Vertical - Z
I	0.968	0.969, 0.985, 0.717	0.880, 0.856, 0.827, **0.257**, 0.940, 0.775
II	0.948	0.932, 0.980, 0.944	0.778, 0.935, **0.089**, **0.166**, 0.962, 0.981
III	0.913	0.964, 0.926, 0.918	**0.170**, 0.795, **0.547**, 0.758, 0.753, **0.445**
IV	0.991	0.936, 0.968, **0.207**	0.904, 0.986, **0.066**, 0.898, 0.995, 0.953
V	0.802	0.866, 0.996, 0.918	0.967, 0.987, 0.902, 0.977, 0.912, 0.692

Figure 20 COH value at the natural frequencies

applied to each element of the matrix $\mathbf{H}(\omega)$, the similarity between the FRFs and their Hilbert transform pairs has been described by the coherence function $\mathrm{COH}(\omega)$ in the Eq.(11). The computed coherence functions are shown in Fig.16

If the bridge behaves linearly, the coherence function should be equal to 1.0 for all frequency ranges of all earthquakes. However, the coherence functions fluctuate along the frequency axis. Moreover, according to the test case (1), it is very hard to observe the similarity among the coherence functions of all earthquakes. This may be the results of two possibilities: (1) there are different non-linear

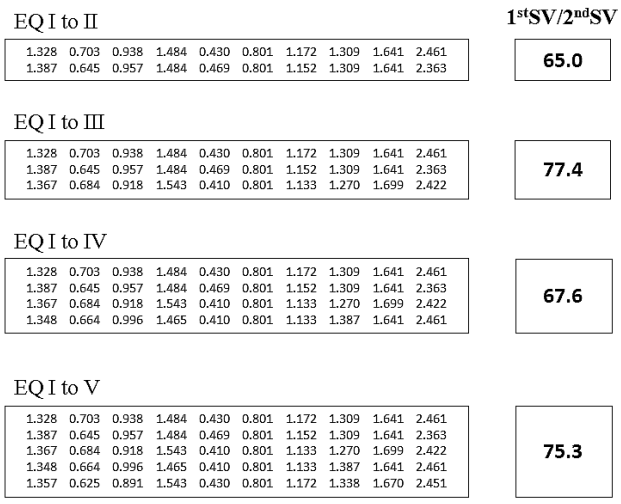

Figure 21 Ratio of the singular value (Healthy)

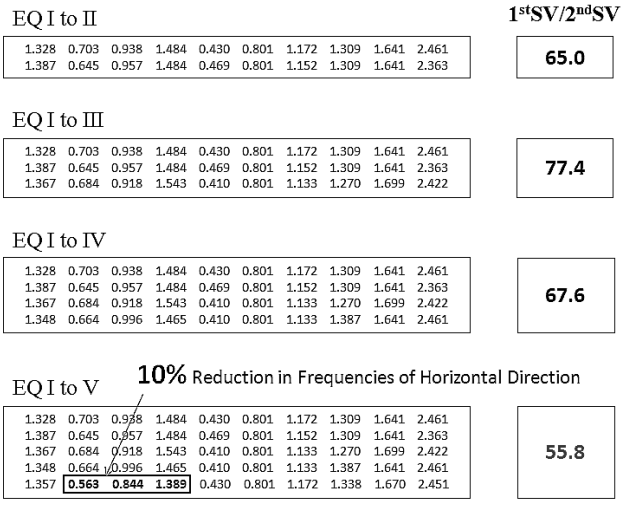

Figure 22 Ratio of the singular value (Damaged)

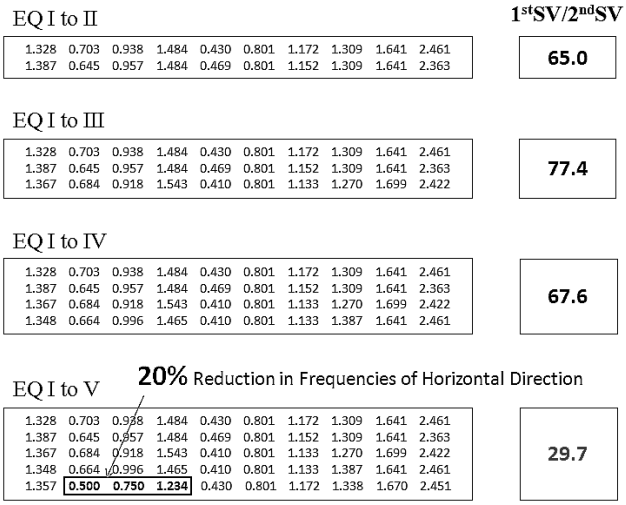

Figure 23 Ratio of the singular value (Damaged)

behaviors occurring during each earthquake, and (2) there are some errors in estimation of the FRFs resulting in the bias estimation on the coherence function. It seems that the approach using the coherence function may not work well. In spite of that, the coherence function can indicate something that may be important. Fig.17 shows the comparison between the CMIFs and the coherence functions. Around the peaks of the CMIFs, the coherence functions are nearly 1.0 for almost all earthquakes. That means the fundamental characteristics governed by the peaks of the FRFs are still nearly linear behavior regardless of earthquake records. The relationship between the coherence function and the natural frequencies will be described again in the next sub-section.

4.3 Natural frequencies extracted from CMIF

By using the method in Section 3.3, the CMIF method extracts the natural frequencies of each record. The extracted natural frequencies are shown in Fig.18. The vertical lines in the figure indicate the natural frequencies that share the same mode shapes in all records. The summary of the values is shown in Fig. 19. The values in the figure show the similarity among all earthquakes. The detection of the similarity will be discussed later.

Regarding the coherence function again, at the extracted natural frequencies, the values of the coherence functions are shown in Fig. 20. Most of the values are almost 1.0 but some of them are very low or almost close to zero. However, the extremely changes in the coherence function for each earthquake are *not* associated with the important peaks in the FRFs such as at 0.801 Hz. This indicates that the main characteristics of the bridge do not change.

The similarity of the obtained natural frequencies can be detected by the feature matrix **F**. For a small number of records, this method may not be useful. But for a large number of records, this method could be used automatically to identify the anomalies. According to the matrix **F** in Eq.(15)-(16), the calculation is perform according to the order of earthquake strike. Also, the effects of changes in the

natural frequencies, which are the results of changes of support conditions or stiffness, will be simulated in order to show the possibilities of the method.

According to the test case (1) where the bridge is healthy, the ratios of the singular values (from now on, will be simply called the ratio) are shown in Fig.21. Firstly if there were two records, the ratio was 65.0. Then, another earthquake (earthquake III) strikes again, the ratio becomes 77.4, and so on until earthquake V. The last value of the ratio after the earthquake V is 75.3. All the ratios are almost the same order. If more records were available, the average or the trend of the ratios would be very beneficial for the comparison.

According to the test case (2) where the bridge is not healthy, the natural frequencies along the horizontal direction (Y) have been decreased by 10% after the earthquake V (Fig.22). The last ratio is 55.8, which is not much lower than previous ratios. This case does not show any significant anomalies.

If the above frequencies are more decreased by 20% after the earthquake V (Fig.23), the last ratio is 29.7, which clearly indicate significant changes in the health condition of the bridge.

5. CONCLUSIONS

Katsushika-Harp Bridge has been monitored for its dynamic behavior for two decades. The problem is how to use these available data to infer the anomalies in the health condition of the bridge. This paper introduces the methods for detecting the anomalies in the health condition. The methods are based on the Frequency Response Functions (FRF) and their derived quantities. The methods use the following damage features: (1) the degree of non-linearity of the vibration calculated from the Hilbert transform of the FRFs, and (2) the natural frequencies extracted from the FRFs. From all available five earthquake records, the proposed methods should indicate that the bridge is still healthy, and should indicate the anomalies if the damages are simulated. The results of the analysis show the following significances:

(1) For the healthy case, the degrees of nonlinearity from all the five earthquake records show not much similarity. However, at the dominant frequencies of the FRFs, the degrees of non-linearity are high regardless of earthquake records. Unfortunately, the non-healthy case could not be tested since lacking of the finite element model of the bridge. Even if the method could detect the anomalies, the characteristics of the anomalies are still not known. More investigation of this method is required.

(2) For the healthy case, the natural frequencies from all the five earthquake records are similar and very stable. For the non-healthy case, the method shows the possibilities to detect the changes in support conditions or stiffness changes. Nevertheless, the method may not detect the local or small changes in the structural properties.

In practice, the success of a monitoring system depends on its predefined “features”, measurement devices with appropriate data interpretation. If the features could be directly measured without imposing any *assumptions*, the monitoring system could possibly work well under an appropriate data interpretation. However, in the case of this paper, a lot of limitations have to be overcome by imposing many assumptions from the beginning of the analysis. Too many assumptions make the results more unreliable. Moreover, the available data is very non-stationary and is highly corrupted by noise. The issues about the accuracy of the proposed methods, and also the complicated damage scenarios simulated by the finite element method must be further investigated.

REFERENCES

Ewins, D.J., 2000. *Modal Testing: Theory, Practice and Application*, Research Studies Press, Baldock, Hertfordshire, England, 300 p.

Kerschen, G., Wordern, K., Vakakis, A.F., and Golinval J.C., 2006. Past, present and future of nonlinear system identification in structural dynamics, *Mechanical Systems and Signal Processing*, 20(2006):505-592.

Michel, C., Guéguen, P., Bard P.V., 2007. Dynamic parameters of structures extracted from ambient vibration measurements: An aid for the seismic vulnerability assessment of existing buildings in moderate seismic hazard regions, *Soil Dynamics and Earthquake Engineering*, (Article in Press).

Rauch, A., Coherence: a powerful estimator of nonlinearity, theory and application, *Proceeding of 10th International Modal Analysis Conference*, San Diego, pp. 784-795, 1992.

Simo, M., and Tomlinson, G.R., 1984. Use of the Hilbert transform in modal analysis of linear and non-linear structures, *Journal of Sound and Vibration*, 96(4):421-436.

Siringoringo, D.M., and Fujino, Y., 2007. Dynamic characteristics of a curved cable-stayed bridge indentified from strong motion records, *Engineering Structures*, 29(2007):2001-2017.

Sohn, H., Farrar, C.R., Hemez, F.M., Shunk, D.D., Stinemates, D.W., and Nadler, B.R., *A Review of Structural Health Monitoring Literature: 1996-2001*, Los Alamos National Laboratory Report, LA-13976-MS, 2003.